

Computational Model for Low Speed Flows Past Airfoils with Spoilers

N. J. Pfeiffer*

Boeing Commercial Airplane Company, Seattle, Wash.

and

G. W. Zumwalt†

Wichita State University, Wichita, Kan.

A computer model has been developed to simulate low-speed flow past an airfoil with a spoiler. An outer solution calculates the potential flow around an effective, closed-wake body. This body is formed by adding to the original airfoil and spoiler geometry: the boundary-layer displacement thickness; a closed wake behind the spoiler; and a trapped vortex at the spoiler hinge. An inner flow solution uses a turbulent jet mixing analysis and conservation of mass and momentum to simulate the time average flow within the wake. The final solution is obtained by iterative matching of the outer and inner solutions.

Nomenclature

c	= airfoil reference chord
C_d	= airfoil section drag coefficient, section drag/(dynamic pressure $\times c$)
C_h	= control surface hinge moment coefficient, section moment about hingeline/(dynamic pressure \times control surface reference chord)
C_l	= airfoil section lift coefficient, section lift/($c \times$ dynamic pressure)
C_m	= airfoil section pitching moment coefficient with respect to the $0.25C_{ref}$ location, section moment/($c \times$ dynamic pressure)
C_p	= coefficient of pressure, $(p - p_\infty)/$ dynamic pressure
e	= edge of the jet mixing region
m	= center of the mixing profile
M	= freestream Mach number
R	= upper recombination streamline
R'	= lower recombination streamline
RN	= Reynold's number
RR'	= streamlines starting at the recombination point
S	= upper separated streamline
S'	= lower separating streamline
S''	= lower streamline with same velocity at trailing edge as S
U	= flow velocity
U_B	= maximum backflow velocity
U_e	= velocity at the local wake edge
$U_{erecomb}$	= edge velocity at recombination
x	= airfoil coordinate parallel to the chord
X	= flow distance from mixing origin
y	= vertical distance from m
α	= angle of attack
δ^*	= boundary-layer displacement thickness
δ_s	= rotation angle of spoiler from nested position
ϕ	= velocity in the mixing region made nondimensional with respect to the local edge velocity

ϕ^*	= velocity in the mixing region referenced to the backflow velocity and made nondimensional with the sum of the backflow and edge velocities
ϕ_B	= nondimensional backflow velocity (u_B/u_e)

I. Introduction

SPOILERS are used widely on aircraft as lateral control devices, as speed brakes, and as lift dumpers during landing. Despite their wide usage, very little theoretical information exists. Almost all design work is done by comparison with experimental results followed by wind tunnel tests of trial models. Wind tunnel tests are not totally reliable due to scale effects and inability in some cases to reduce surface details to model size accurately. Costly flight test programs may be required in some cases to produce desired results.

An accurate computational model has been developed to aid the design of spoilers. This model can compute the surface pressures on an airfoil spoiler combination in steady, incompressible, two-dimensional flow. Force and moment coefficients are obtained by integration of pressures and skin friction.

II. Flow Description

The first step in the model development was to use flow visualization techniques to determine the pattern of flow caused by the spoiler. The flow was examined using both a water table and oil streaks on a flow-splitter plate mounted on a wind tunnel model.

These examinations indicate that the wake has two main characteristics. First, it has an unsteady nature due to a shed vortex street. Second, despite this periodic behavior, there is a region of wake that remains nearly constant in shape and closes a short distance downstream of the trailing edge. The shedding of vortices may have considerable effect on other surfaces in the path downstream, but the time average flow pattern obtained by using the splitter plate (Fig. 1) indicates that these perturbations may be neglected if only time average effects are required.

Figure 1 represents the flow on the splitter plate as investigated by Wentz and Ostowari.¹ It clearly shows two basic regions: first, an outer essentially potential flow region, and second, a near wake region behind the spoiler. The figure also shows that the near wake may be subdivided into two more

Presented as Paper 81-0253 at the AIAA 19th Aerospace Sciences Meeting, St. Louis, Mo., Jan. 12-15, 1981. Submitted March 3, 1981; revision received June 29, 1981. Copyright © American Institute of Aeronautics and Astronautics, Inc., 1981. All rights reserved.

*Specialist Engineer, Flight Controls Research. Member AIAA.

†Distinguished Professor, Department of Aeronautical Engineering. Associate Fellow AIAA.

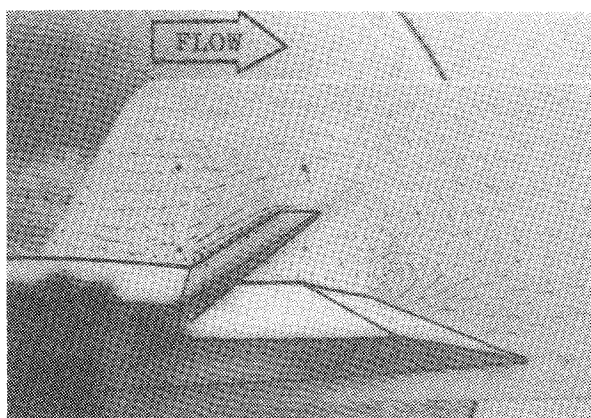


Fig. 1 Oil drop flow visualization; $\alpha=0$ deg, $\delta_s=40$ deg, $M=0.13$, $RN=2.2 \times 10^6$.

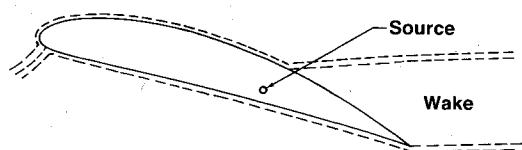


Fig. 2 Infinite wake produced by added source.

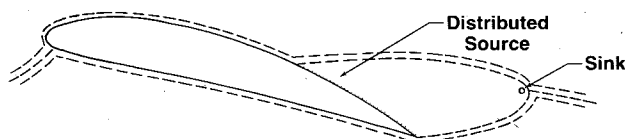


Fig. 3 Finite wake produced by added source and sink.

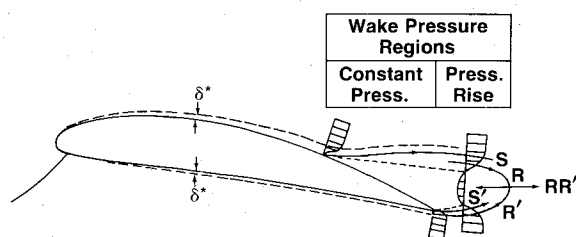


Fig. 4 The Zumwalt-Naik model.

parts. The part upstream of the wing trailing edge shows very little fluid motion and thus may be assumed to be at nearly constant pressure. The part downstream of the trailing edge is characterized by a pair of vortices; the upper one rotating clockwise (for left to right flow) and a smaller one below it rotating counterclockwise. The streamline between these two vortices extends from a downstream stagnation point which defines the end of the wake. It should be noted that the backflow velocity along the line between the vortices is a sizeable fraction of the local velocity at the edge of the wake. Due to the magnitude of this backflow velocity, it would seem prudent to include some model of this wake flow in the overall solution of the problem.

III. Previous Related Investigations

The spoiler flow problem is a specific case within the general topic of separated flows. Separated flows have been of interest ever since it was found that classical potential-flow theory would not describe adequately such simple cases as a cylinder or a plate held normal to a uniform flow. Several models have been suggested and developed to simulate the separated flow behind an airfoil without a spoiler.

A method was developed by Jacob^{2,3} and was modified subsequently by others.⁴⁻⁶ These models add a source or source distribution to the aft portion of the airfoil to simulate a separated wake (Fig. 2). This produces a wake that extends to infinity downstream. This infinite wake, however, conflicts with experimental observations that the wake closes a short distance downstream from the trailing edge.⁷

A more recent model by Jacob⁸ adds a sink downstream to close the wake region (Fig. 3). This model is physically more realistic for the flow outside of the body and wake region, but it still does not account for any of the flow parameters within the wake region.

Zumwalt⁹ and Gross¹⁰ both postulated flow models that were derived by extending supersonic jet-mixing theory to incompressible flow. Jet-mixing theory was first studied for supersonic flows because, 1) supersonic flows have no vortex street extending downstream to complicate the problem, and 2) there is a simple relation between flow properties and flow direction. A simple back-step in subsonic flow also has no vortex shedding and thus was studied. Nash¹¹⁻¹³ described much of the experimental and analytic work dealing with jet-mixing theory applied to these problems. Zumwalt and Naik extended this previous work by assuming that the wake could be closed for subsonic airfoils, and the basic pressure distribution on the airfoil and near wake would not be greatly influenced by the vortex shedding downstream. A general diagram of the Zumwalt-Naik model is shown in Fig. 4. This model differs from previous ones in that it is composed of an iterative solution of two parts; an outer flow solution and an inner flow solution.

The outer flow problem involves the flow around an effective body. The effective body is formed by adding the closed wake to the fixed airfoil geometry. The solution for this problem is a combination of potential and boundary-layer solutions on the fixed surface, coupled with a potential flow solution for a defined pressure distribution on the free wake surface.

The inner flow problem describes the flow within the closed wake. Mixing velocity profiles are developed and mass balances are made. The solution of these yields an updated value of the pressure at the back of the wake. Iterations are then made between inner and outer solutions until a convergence is reached.

The validity of this model was demonstrated by experimental pressure and velocity measurements collected by Seetharam.⁷ This model accurately calculated the pressure distribution and separation point location for a GA(W)-1 airfoil at high angles of attack.

IV. Spoiler Flow Model

The basis of the spoiler flow model is the matching of solutions for the outer and inner regions. The outer solution describes the flow past a closed body formed by adding to the airfoil shape 1) the boundary-layer displacement thickness, 2) a possible separation bubble ahead of the spoiler (with or without reattachment to the spoiler), and 3) a closed wake behind the spoiler. The inner solution computes the flow for the interior of the near wake. These are solved iteratively until they are compatible.

Outer Solution

The outer solution requires a potential flow routine of the mixed boundary condition type. A routine using surface vortex panels¹⁴ was used. For the portion where flow is attached, surface coordinates are input and zero normal velocity is imposed as the boundary condition. For the separated flow portions, a pressure distribution must be specified and an initial trial wake shape assumed. This wake pressure distribution yields the tangent velocity along the wake. The trial wake shape is modified through iterations within the potential flow routine which attempt to match the wake shape to the local tangent velocity.

The wake pressure distribution is considered to be constant from the separation point to the trailing-edge plane. The pressure then increases along the upper and lower wake surfaces to the recombination point. This produces a nonlifting wake. The pressure rise function is defined so that a family of similar curves exist for variations in trailing edge and recombination pressures. Both of these pressures may change throughout the iterative solutions of the inner and outer flows.

The boundary layer is handled as a simple laminar approximation¹⁵ up to a fixed transition. Transition is assumed to occur at just past 5% on the upper side, and just past 10% on the lower side. A modified Truckenbrodt turbulent boundary-layer method¹⁵ is used following transition. The displacement thickness is added to the airfoil geometry in order to produce an effective body.

The presence of a spoiler creates a problem due to the sharp concave corner at the hinge. A potential flow program alone would attempt to stagnate the flow at this corner. For very small spoiler deflections, the boundary layer will smooth the sharp corner and allow the potential flow routine to function realistically. However, as the spoiler deflection increases (greater than 10-15 deg), the boundary layer near the hinge becomes quite thick and may become unstable. When this occurs, the flow separates from the airfoil ahead of the hinge line and may reattach somewhere along the projected spoiler, or at high angles of attack it may leave the spoiler within a larger separation region.

This spoiler hinge bubble is modeled by finding a separation point on the airfoil and a reattachment point on

the spoiler. The separation point is defined to be the point where the turbulent boundary-layer shape factor H becomes greater than 1.8. This value is within the generally accepted range of shape factors at separation and best matches the observed experimental results. The reattachment point is assumed to be the point on the spoiler that has a pressure coefficient equal to that at the separation point on the airfoil. A parabolic curve is passed through these points so that it is tangent at the separation point. If no point on the spoiler has as low a pressure as that of the separation point, general upstream separation is assumed to have occurred. The wake then starts at the new separation point and engulfs the spoiler.

The separation point, in the case of a general separation, is allowed to move during successive potential boundary-layer iterations until it settles. The location of this point is determined by matching a series of criteria that include the H shape factor, the shape factor Γ developed by Buri,¹⁵ and a C_{ps} term presented by Goldschmied.¹⁶

Inner Solution

The basic purpose of the inner flow calculations is to provide a revised value for the pressure coefficient at the wake recombination point. This value in turn is used in the outer flow calculations through the revised pressure distribution on the wake.

The flow within the wake can be described by defining a few streamlines and the trailing-edge plane velocity profile. These are presented in Fig. 5. Streamlines S and S'' are the separating streamlines, and define the outer boundary of the wake flow. Streamlines R and R' are the recombination streamlines which stagnate at a common point near the back

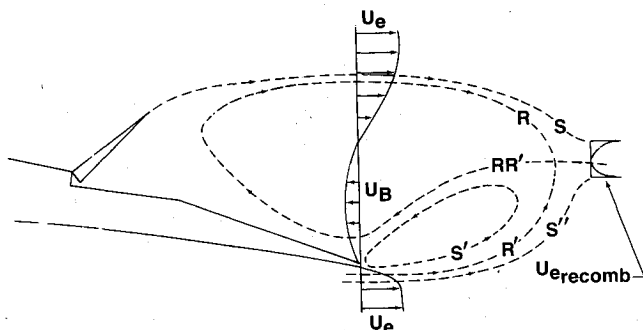


Fig. 5 The spoiler wake model.

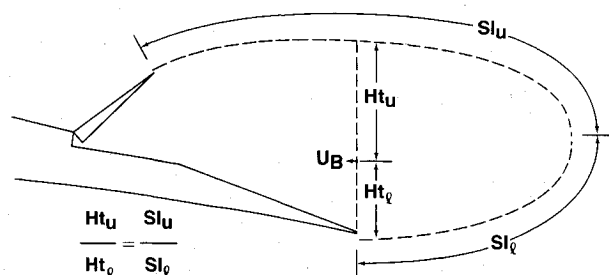


Fig. 8 Location of the maximum backflow.

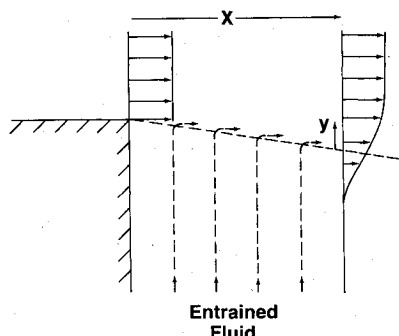


Fig. 6 Mixing of a jet flow with a large volume of fluid.

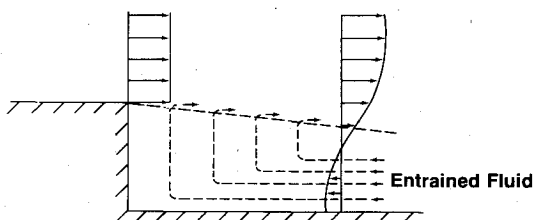


Fig. 7 Mixing of a jet flow with a restricted volume of fluid.

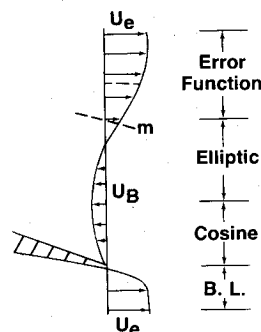


Fig. 9 Velocity profile at the trailing-edge plane.

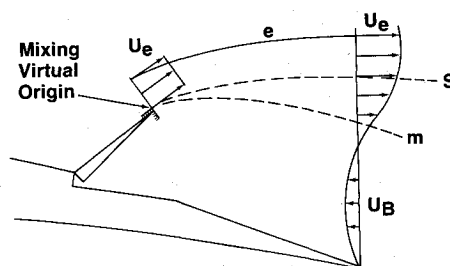


Fig. 10 Front wake mixing region.

of the wake bubble. The RR' streamline originates at this stagnation point and extends both upstream and downstream. The S' streamline is the trailing-edge separation streamline which forms a small recirculation bubble just downstream of the trailing edge. The velocity profile above the airfoil at the trailing-edge plane varies from the edge velocity U_e to the maximum backflow velocity U_B , and back to zero at the airfoil surface. Below the airfoil, the flow velocity may be described by the appropriate turbulent boundary-layer profile with the same edge velocity U_e as above.

Care was taken to model the trailing-edge plane velocity profile above the airfoil, in a fashion consistent with both theory and experimental measurements. Korst¹⁷ developed a theory of turbulent jet-mixing in regions of constant pressure. He derived a velocity profile defined by the error function in the following way:

$$\phi = U/U_e = \frac{1}{2} \left[1 + \operatorname{erf} \left(\sigma \frac{y}{X} \right) \right] \quad (1)$$

where U is the velocity, U_e the edge velocity, y the distance from the middle of the profile, X the distance from the origin of the mixing region, and σ the jet spreading rate parameter (Fig. 6). The value for σ is well established experimentally for incompressible flow, and equals 12.

The Korst model is completely appropriate only when the jet exhausts into a very large volume. This allows an essentially infinite source of fluid to supply the mass required by the entrainment of the jet. If the jet exhausts into a restricted volume (Fig. 7), there must be a finite backflow velocity in order to satisfy continuity. A general expression for a modified velocity profile similar to that of the original Korst profile but including backflow velocity, U_B , is

$$\phi = \frac{1}{2} \left[(1 - \phi_B) + (1 + \phi_B) \operatorname{erf} \left(\sigma \frac{y}{X} \right) \right] \quad (2)$$

where

$$\phi_B = U_B/U_e$$

A second dimensionless velocity ϕ^* may be defined as follows:

$$\phi^* = \frac{\phi + \phi_B}{1 + \phi_B} = \frac{1}{2} \left[1 + \operatorname{erf} \left(\sigma \frac{y}{X} \right) \right] \quad (3)$$

This definition has the effect of moving the reference velocity line from zero to the backflow velocity. The value of the jet spreading rate parameter σ is also affected by the backflow velocity.¹⁸ The simple incompressible value may be extended to one with a finite backflow by making

$$\sigma = 12 [(1 - \phi_B) / (1 + \phi_B)] \quad (4)$$

The velocity profiles described so far both have the same shape above and below a line m through the middle of the profile. The modified profile matches experimental data for separated airfoils in the region above the middle of the profile, but not below the midpoint.

The original Korst flow is essentially the mixing of a uniform jet with another uniform flow. This produces a profile which must be similar above and below the center of the mixing region. The actual flow for a separated airfoil corresponds to the mixing of an almost uniform jet with an elongated vortex. This does not produce a mixing profile that maintains the same characteristic shape above and below the center of the profile. The upper portion of the profile is well modeled by the modified error function profile given earlier. The lower portion may be modeled better by a portion of an ellipse. This elliptic curve starts tangent to the error function curve and terminates vertically at the point of maximum backflow. Therefore, the location of the maximum backflow

velocity U_B must be determined. If the size of the vortices in the wake are considered to be proportional to the lengths of the wake shear surfaces that drive them, then the location of this maximum backflow velocity is proportional to the ratio of these wake surface lengths (Fig. 8). The final portion of the velocity profile is well matched by a quarter of a cosine curve (Fig. 9).

The inner solution calculations are started by assuming a trial value of ϕ_B . The computation procedure that follows is divided into four parts, three of which are iterative loops.

Part 1 is the S streamline loop. This section defines the mixing profile at the trailing edge including the locations of the m and S lines (Fig. 10). This is accomplished by enforcing continuity on two control volumes. First, the mass entering the control volume between the S streamline and an arbitrary edge streamline e at the spoiler tip, must equal the mass leaving between the same streamlines at the trailing-edge plane. Second, a control volume is defined to be the region below the S streamline, behind the spoiler, above the airfoil, and in front of the trailing-edge plane. Continuity on this control volume implies that the mass flow through the trailing-edge plane from the airfoil to the streamline S must equal zero.

Part 2 is the R streamline loop. This loop establishes the velocity and locations of the R and R' streamlines by using a mass balance. The rate of mass scooped into the wake between the airfoil and the streamline R' below it, must equal the rate of mass ejected between the R and S streamlines at the trailing-edge plane.

Part 3 is the recombination loop. This loop uses the momentum equation in the flow direction on the rear wake bubble to establish a value for the recombination pressure coefficient $C_{precomb}$ (Fig. 5). The sum of the distributed pressure force on the rear of the wake is set equal to the sum of the rates of change of momentum on the trailing-edge plane, from the S'' streamline up to the S streamline, minus the rate of momentum loss out the back of the wake.

Part 4 is the recompression check. Nash¹² developed a recompression analysis based on empirical results. He defined a quantity often called the Nash factor and established it as a function of Mach number. This factor is calculated using quantities from parts 1-3 and then compared with the empirical value. If the two values do not match, a new value of ϕ_B is assigned and parts 1-4 are repeated until there is a convergence to the empirical value of the Nash factor.

Final Convergence and Calculations

The new recombination pressure coefficient is checked with the previous value, which was used in the outer flow solution. Iterations between the inner and outer solutions are continued

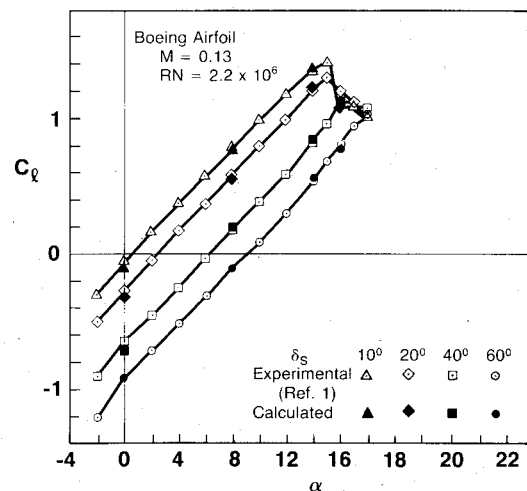


Fig. 11 Comparison of lift for the Boeing airfoil.

until these pressure coefficient values converge. The potential flow routine is then called one last time to do final smoothing on the wake, and the results are printed out.

The end result of the computation procedure is the calculation of a pressure distribution around an airfoil and spoiler. The forces and moments on the body are found by integrating functions of the pressure distribution over the surface of the body. Corrections to the forces are then made for skin friction by using the Squire-Young method.¹⁵

V. Results and Discussion

Results were calculated for two airfoils for which detailed data exist for flow with spoilers. The first was an 11.3% thick Boeing airfoil with a 15.7% chord spoiler hinged at 73.3% of the airfoil chord. The experimental results of Wentz and Ostowari¹ were available for this airfoil. The second was a 13% thick LS(1)-0413 airfoil with a 10% chord spoiler hinged at 77.5% of the airfoil chord. The experimental results of Rodgers et al.^{19,20} were available for this airfoil. Force and moment coefficients for the Boeing airfoil are plotted in Figs. 11-14 and a typical pressure distribution is plotted in Fig. 15. Similar plots for the LS(1)-0413 airfoil are presented in Figs. 16-20.

Calculated pressure distributions and force and moment results correlate well with the experimental values. Results for extreme cases indicate that the model gives reasonable results for spoilers deflected from 2.5 to 90 deg. Preliminary results for the 0-deg spoiler deflection case, which corresponds to simple airfoil separation due to angle of attack, have been quite promising (Fig. 21).

The current computer code has three limitations: 1) it includes no compressibility corrections, 2) only fixed boundary-layer transition is considered, and 3) there is no calculation of either short or long bubble laminar separation. Therefore, the

code presently is restricted to incompressible flow and conditions that do not promote laminar flow or laminar separations. It should be noted that Reynold's number effects on transition are not applicable, due to the fixed transition constraint, but the effect on turbulent boundary-layer buildup is modeled. Any of the preceding limitations could be eliminated with a reasonable amount of effort.

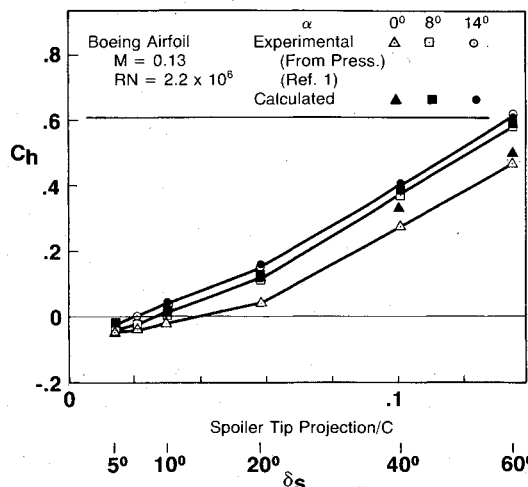


Fig. 14 Comparison of spoiler hinge moment for the Boeing airfoil.

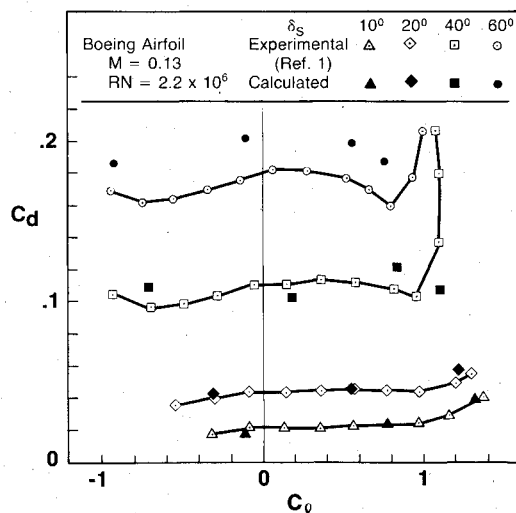


Fig. 12 Comparison of drag for the Boeing airfoil.

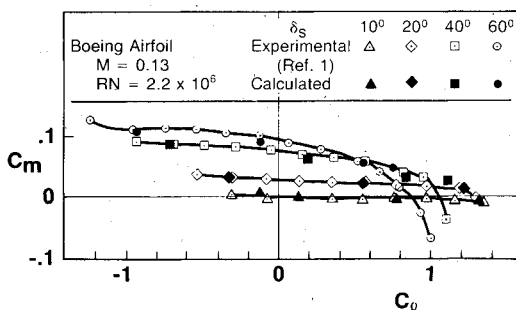


Fig. 13 Comparison of moment for the Boeing airfoil.

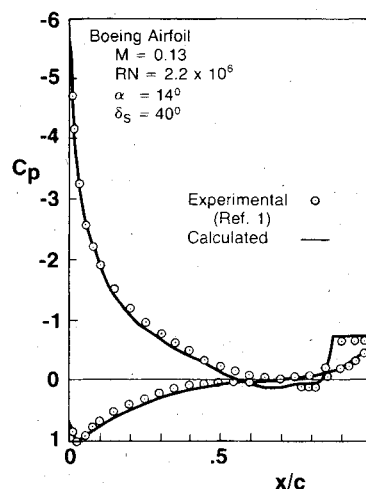


Fig. 15 Comparison of a pressure distribution for the Boeing airfoil.

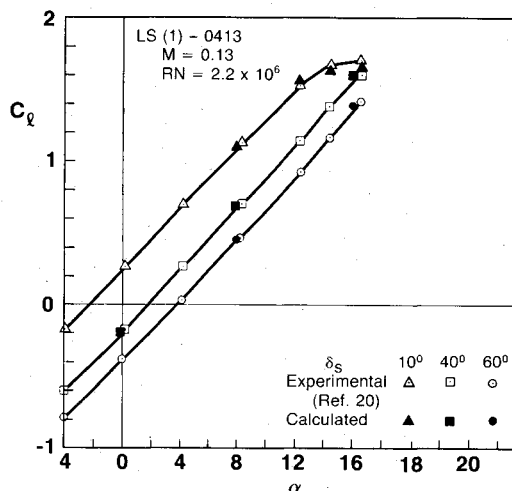


Fig. 16 Comparison of lift for the LS(1)-0413 airfoil.

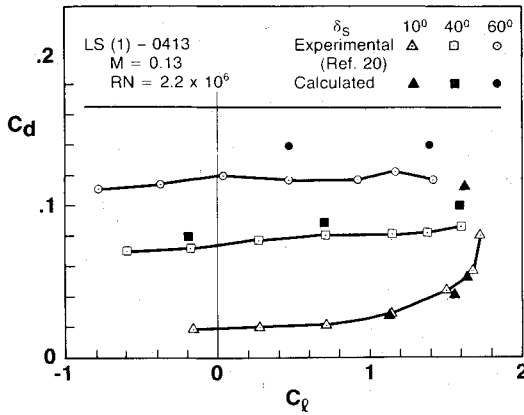


Fig. 17 Comparison of drag for the LS(1)-0413 airfoil.

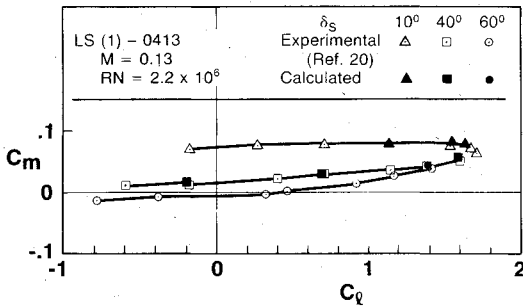


Fig. 18 Comparison of moment for the LS(1)-0413 airfoil.

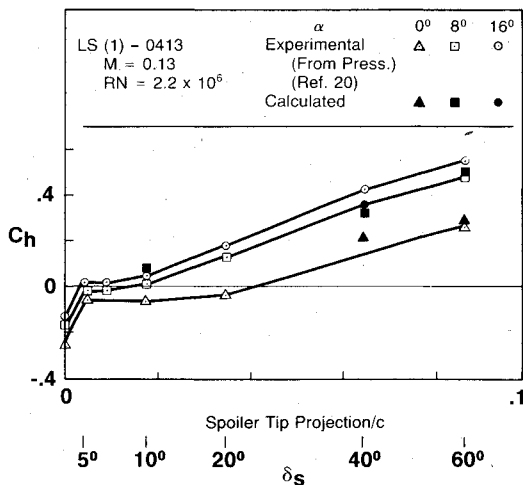


Fig. 19 Comparison of spoiler hinge moment for the LS(1)-0413 airfoil.

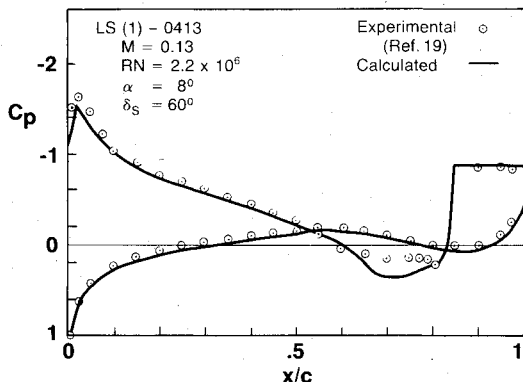


Fig. 20 Comparison of a pressure distribution for the LS(1)-0413 airfoil.

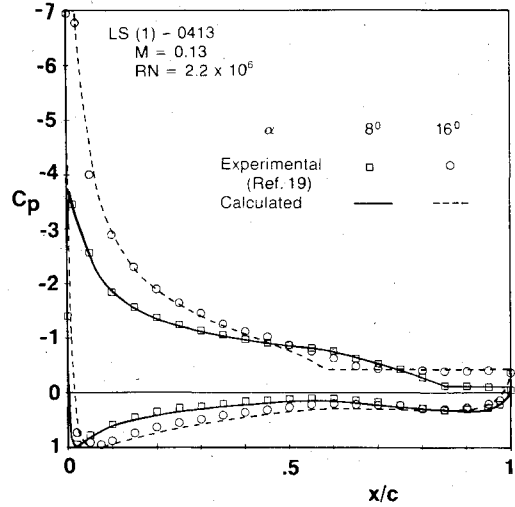


Fig. 21 Comparison of pressure distributions for the LS(1)-0413 airfoil with nested spoiler.

All computations have been carried out on an IBM System 370, model 3031. CPU time on this machine for a single angle of attack and spoiler deflection is typically less than 3 min.

VI. Conclusion

A flow model has thus been formulated which 1) includes the physically significant features, and 2) requires no a priori knowledge of wake shape, pressure, or separation ahead of the spoiler.

Acknowledgments

This model was developed in conjunction with an experimental study at Wichita State University directed by Professor W. H. Wentz Jr. Both the analytical and experimental studies were funded by the Boeing Commercial Airplane Company.

References

- Wentz, W. H. Jr. and Ostowari, C., "Effects of Design Variables on Spoiler Control Effectiveness, Hinge Moments and Wake Turbulence," AIAA Paper 81-0072, Jan. 1981.
- Jacob, K., "Computation of Separated Incompressible Flow Around Airfoil and Determination of Maximum Lift," Lecture at WLGR Committee Meeting for Aerodynamics, Institute of Technology, Berlin, AVA Rept. 67A62, Oct. 1-4, 1967; publication in *Zeitschrift für Flugwissenschaften*, July 1969.
- Jacob, K. and Steinbach, D., "A Method for Prediction of Lift for Multi-Element Airfoil Systems with Separation," Paper 12, AGARD CP-143, 1974.
- Hahn, M., Rubbert, P. E., and Mahal, A. S., "Evaluation of Separated Flow Criteria and Their Application to Separated Flow Analysis," Tech. Rept. AFFDL-TR-145, Jan. 1973.
- Bhatley, I. C. and McWhirter, J. S., "Development of Theoretical Method for Two-Dimensional Multi-Element Airfoil Analysis and Design, Part I, Viscous Flow Analysis Method," AFFDL-12-96, Aug. 1972.
- Farn, C. L. S., Goldschmied, F. R., and Whirlow, D. K., "Pressure Distribution Prediction for Two-Dimensional Hydrofoils with Massive Turbulent Separation," *Journal of Hydrodynamics*, Vol. 10, July 1976, pp. 95-101.
- Seetharam, H. C., "Experimental Investigation of Separated Flow Fields on an Airfoil at Subsonic Speeds," Ph.D. Dissertation, Wichita State Univ., AR 75-1, 1975.
- Jacob, K., "Weiterentwicklung eines Verfahrens zur Berechnung der abgelösten Profilstromung mit besonderer Berücksichtigung des Profiwiderstandes," DFVLR-AVA Internal Rept. 251-75A16, June 1975.
- Zumwalt, G. W. and Naik, S. N., "An Analytical Method for Highly Separated Flow on Airfoils at Low Speeds," NASA-CR-145249, May 1977.

¹⁰Gross, L. W., "The Prediction of Two-Dimensional Airfoil Stall Progression," AIAA Paper 78-155, Jan. 1978.

¹¹Nash, J. F., "A Review of Research on Two-Dimensional Base Flow," Aeronautical Research Council R&M 3323, March 1962.

¹²Nash, J. F., "An Analysis of Two-Dimensional Turbulent Base Flow, Including the Effect of the Approaching Boundary Layer," Aeronautical Research Council R&M 3344, July 1962.

¹³Nash, J. F., "Experiments on Two-Dimensional Base Flow at Subsonic and Transonic Speeds," Aeronautical Research Council R&M 3427, Jan. 1963.

¹⁴Maskew, B., "INVERSE Program," Analytical Methods, Inc., Bellevue, Wash., 1979.

¹⁵Schlichting, H., *Boundary Layer Theory*, McGraw-Hill, New York, 1960.

¹⁶Goldschmied, F. R., "An Approach to Incompressible Separation under Adverse Pressure Gradients," *Journal of Aircraft*, March-April 1965, p. 108.

¹⁷Korst, H. H., "A Theory for Base Pressures in Transonic and Supersonic Flow," *Journal of Applied Mechanics*, Vol. 23, Dec., 1956, p. 593.

¹⁸Korst, H. H. and Chow, W. L., "Non-Isoenergetic Turbulent ($P_r = 1$) Jet Mixing Between Two Compressible Streams at Constant Pressure," Univ. of Illinois, ME-TN-393-2, April 1965.

¹⁹Rodgers, E. J., Wentz, W. H., and Ostowari, C., "Experimental Studies of Pressure Distributions and Flow Fields on the GA(W)-2 Airfoil Incorporating a Flap and Spoiler," Wichita State Univ., AR 79-4, July 1979.

²⁰Wentz, W. H., "Wind Tunnel Test of the GA(W)-2 Airfoil with 20% Aileron, 25% Slotted Flap, 30% Fowler Flap, and 10% Slot-Lip Spoiler," Wichita State Univ., AR 76-2, Aug. 1976.

From the AIAA Progress in Astronautics and Aeronautics Series...

ENTRY HEATING AND THERMAL PROTECTION—v. 69

HEAT TRANSFER, THERMAL CONTROL, AND HEAT PIPES—v. 70

Edited by Walter B. Olstad, NASA Headquarters

The era of space exploration and utilization that we are witnessing today could not have become reality without a host of evolutionary and even revolutionary advances in many technical areas. Thermophysics is certainly no exception. In fact, the interdisciplinary field of thermophysics plays a significant role in the life cycle of all space missions from launch, through operation in the space environment, to entry into the atmosphere of Earth or one of Earth's planetary neighbors. Thermal control has been and remains a prime design concern for all spacecraft. Although many noteworthy advances in thermal control technology can be cited, such as advanced thermal coatings, louvered space radiators, low-temperature phase-change material packages, heat pipes and thermal diodes, and computational thermal analysis techniques, new and more challenging problems continue to arise. The prospects are for increased, not diminished, demands on the skill and ingenuity of the thermal control engineer and for continued advancement in those fundamental discipline areas upon which he relies. It is hoped that these volumes will be useful references for those working in these fields who may wish to bring themselves up-to-date in the applications to spacecraft and a guide and inspiration to those who, in the future, will be faced with new and, as yet, unknown design challenges.

Volume 69—361 pp., 6×9, illus., \$22.00 Mem., \$37.50 List
Volume 70—393 pp., 6×9, illus., \$22.00 Mem., \$37.50 List

TO ORDER WRITE: Publications Dept., AIAA, 1290 Avenue of the Americas, New York, N.Y. 10104